Characterization of Ternary Mg–Sn–Mn Alloys

A.E. Gulec*, Z.C. Oter, K.O. Gunduz, M. Tarakci and Y. Gencer

Gebze Technical University, Department of Materials Science and Engineering, 41400 Gebze, Kocaeli, Turkey

Ternary Mg–2Sn–Mn (0.5, 1, 2, and 2.5 wt% Mn) alloys were prepared under vacuum/argon atmosphere controlled furnace to investigate their microstructural and mechanical properties as a potential biodegradable implant material. As-cast alloys were heat treated at 550 °C for 24 h and then at 300 °C for 16 h. The alloys were characterized as-cast and after the heat treatment by optical microscopy, scanning electron microscopy, X-ray diffraction, and microhardness measurement. Mg phase is evident for both as-cast and heat-treated alloys while Mg_2Sn intermetallic phase is detected in all heat treated alloys except Mg–2Sn–0.5Mn. The dendritic microstructure changed to a microstructure with equiaxed grains after the heat treatment. The increase of Mn in ternary Mg–2Sn–Mn alloys resulted in a microstructure composed of smaller grains. Moreover, microhardness of ternary alloys slightly increased with the addition of Mn.

1. Introduction

Magnesium, having a density 1.74 g/cm^3, is the lightest among the structural materials used in engineering applications and widely preferred in automotive and aerospace applications owing to their excellent strength to weight ratio, good electromagnetic shielding, superior damping capacity and good castability. Reducing the weight of vehicles will decrease the fuel consumption which will also lower the emission of greenhouse gases such as CO_2 [1–5]. As a result of their dissolubility in chloride containing aqueous solutions, magnesium is a potential biodegradable implant material and unlike the titanium based implant materials, biodegradable magnesium alloys do not require a second surgical operation for the removal process and are mechanically more compatible with natural bone by virtue of their similar elastic modulus values (Mg alloys: 40–45 GPa, bone: 10–40 GPa) [6, 7]. Magnesium itself is an essential mineral for the body and responsible for corporation of calcium into the bone. Consequently releasing of magnesium ions during the dissolution process is beneficial for the healing process of bones [8]. However poor corrosion and wear resistance of magnesium and its alloys limit their application areas [3–5, 9–11]. Therefore to improve the properties of magnesium addition of alloying elements is highly required [12, 13].

One of the extensively used alloying elements in magnesium is aluminum. However aluminum containing magnesium alloys are serviceable only at room temperature and for biomedical applications it is proven that aluminum is toxic for the body causing dementia and Alzheimer disease [14, 15]. Therefore another requirement emerges for biomedical applications that alloying elements used in magnesium should not harm body caus-

ing toxic or allergic reactions. Tin and manganese are important alloying elements used in magnesium alloys to improve the mechanical and corrosion resistance of magnesium. Addition of tin increases the creep resistance of magnesium alloys due to formation of an intermetallic compound (Mg_2Sn) which melts at elevated temperature (770 °C) [16]. A study made by Zhao showed that tin addition up to 3 wt% did not cause any toxicity in Mg63 cells and improved the mechanical properties drastically [17]. Manganese addition into the magnesium alloys does not affect the tensile strength but improves the yield strength slightly, however the most important function of manganese addition is to increase resistance of the Mg alloys in salt water by forming harmless intermetallic compounds with impurities [18]. A study made by Xu showed that manganese addition into magnesium did not cause any toxicity in human body [19]. Therefore addition of tin and manganese is very beneficial for magnesium alloys. This study focuses on production and characterization of a new potential biomedical alloy of Mg–2Sn–xMn ($x = 0.5, 1, 2, 2.5$ wt%).

2. Experimental

Pure magnesium, pure tin and pure manganese with 99.95% purity were used to produce ternary alloys with targeted compositions given in Table I. The alloy ingots were prepared by using induction furnace under Ar (99.99% pure) atmosphere to prevent oxidation, cast into water cooled copper molds and quenched in water. Each ingot was sliced into two pieces (top and bottom) to obtain average chemical analysis from different regions using mass spectroscopy. The solution treatment was carried out at 550 °C for 24 h and then ageing treatment at 300 °C for 16 h for the alloys. The phase analysis was carried out using X-ray diffraction (XRD) (Rigaku D-Max 2200) in 10°−90° range with 2°/min scan rate. A further XRD analysis was carried out between 10° and 40° with 0.5°/min scan rate for the same alloys for detecting low

———————

*corresponding author; e-mail: egulec@gtu.edu.tr

intensity diffraction peaks. Instron Wolpert 2100 microhardness tester was used for the Vickers microhardness measurements of the alloys by applying a load of 100 g for 5 s with 300 μm distance between measurements. The surfaces of the alloys were ground using 80–1200 SiC papers sequentially and then polished using colloidal silica. The polished samples were etched using a solution containing 1 ml nitric acid, 20 ml acetic acid, 20 ml deionised water and 60 ml ethylene glycol, rinsed in deionised water and then in ethanol and dried with warm air. The microstructures of alloys were examined using an optical microscope.

TABLE I

Chemical composition [wt.%] of targeted Mg–Sn–Mn ternary alloys a1–a4.

element	a1	a2	a3	a4
Mg	97.5	97	96	95.5
Sn	2	2	2	2
Mn	0.5	1	2	2.5

3. Results and discussion

The chemical analysis results of the Mg–Sn–Mn ternary alloys obtained by optical emission spectroscopy are given in Table II. The results given in Table II shows that the chemical composition of each alloy was slightly different compared to the aimed compositions given in Table I. Trace amounts of impurities such as Al, Si, and Nd in metals are detected. Therefore the impurities are negligible. The results show that Mg–Sn–Mn alloys were produced in parallel to the targeted chemical compositions by induction melting method under controlled argon atmosphere. Furthermore, the results show that the samples are considerably homogeneous as there is no big difference between bottom and top sections of the cast Mg–Sn–Mn alloys.

TABLE II

Chemical analysis [wt.%] of the prepared Mg-Sn-Mn alloys a1–a4, top and bottom.

alloy	Mg	Sn	Mn	Al	Si	Nd
a1b	97.69720	1.71564	0.50038	0.05280	0.01153	0.00605
a1t	97.66514	1.75117	0.49668	0.05156	0.01186	0.00583
a2b	97.11439	1.61771	1.17634	0.05081	0.01421	0.01001
a2t	97.06767	1.61792	1.21888	0.05127	0.01459	0.01119
a3b	96.39413	1.64756	1.87556	0.04666	0.01578	0.00178
a3t	96.27658	1.70538	1.92308	0.05142	0.01685	0.01119
a4b	95.78834	1.62326	2.48801	0.05097	0.01772	0.01493
a4t	95.84303	1.61244	2.45400	0.04997	0.01751	0.01058

The XRD analysis results of the Mg–Sn–Mn alloys in as-cast state and after the heat treatment are given in Fig. 1. The XRD spectrum shows that only Mg phase is evident for the as-cast alloys while there was not any intermetallic phase. However, Mg_2Sn intermetallic phase is detected for alloy 2, alloy 3 and alloy 4 in addition to Mg phase after the heat treatments. Mg_2Sn phase formation was prevented from the rapid cooling of the alloys in as-cast state. However, the solid solution treatment at 550 °C for 24 h and then the ageing treatment at 300 °C for 16 h resulted in Mg_2Sn intermetallic phase formation in grain boundaries and in grains. Mg is the only phase formed both in as-cast state and after the heat treatment of the alloy 1. XRD intensities of the phases which are detected after the heat treatment are relatively higher than those of the as-cast alloys.
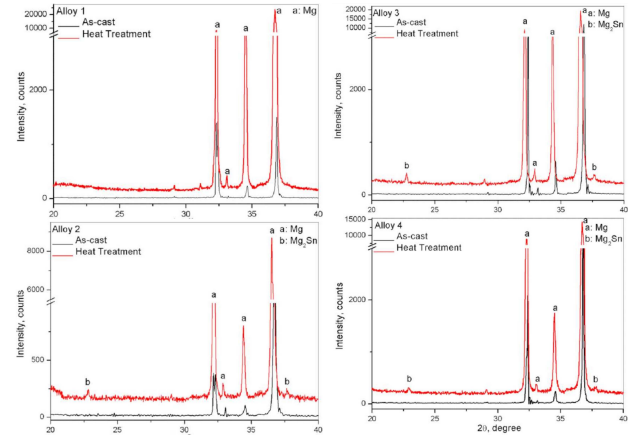
Fig. 1. XRD analysis of Mg–Sn–Mn ternary alloys as cast and heat treated.

Figure 2 shows the microstructure of the Mg–Sn–Mn ternary alloys obtained by optical microscopy. Typical dendritic structures dominate the microstructures. The length of dendrite arms varies with Mn amount in the ternary alloys. The longest dendrite arms were seen in Fig. 2a while the arms became shorter in Fig. 2b and d. The dendrites arms are of the same range of length in Fig. 2a while structure of the matrix is similar to that of the other alloys. Alloy 3 has a different microstructure compared to the other alloys. Alloy 3 has equiaxed microstructures instead of dendritical structures (Fig. 2c). The slight difference in microstructures may be attributed to the chemical difference of the alloys.

The optical micrographs of Mg–Sn–Mn ternary alloys after the heat treatment were given in Fig. 3a–d. The grain boundaries were clearly seen and equiaxed grain structure was evident for the heat treated alloys. The grain size was changed with Mn amount in the Mg–Sn–Mn ternary alloys. The grain size decreased with the increase of Mn content in the alloys. The grain size was measured as approximately 400 μm in alloy 1 (Fig. 3a) while it decreased to 70–80 μm in alloy 4 (Fig. 3d). It may be concluded that Mn has a grain reduction effect on heat treated Mg–Sn–Mn ternary alloys.

The SEM micrographs of as-cast Mg–Sn–Mn ternary alloys are given in Fig. 4 with a portion of their magnified images. The microstructures obtained by SEM are sim-
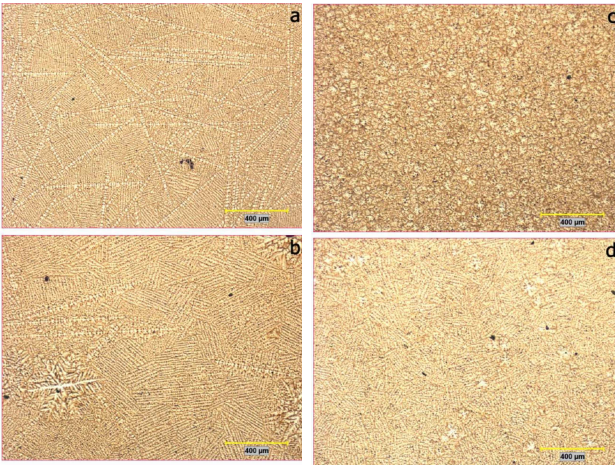
Fig. 2. Optical micrographs of as cast treated Mg–Sn–Mn ternary alloys: (a) alloy 1, (b) alloy 2, (c) alloy 3, and (d) alloy 4.
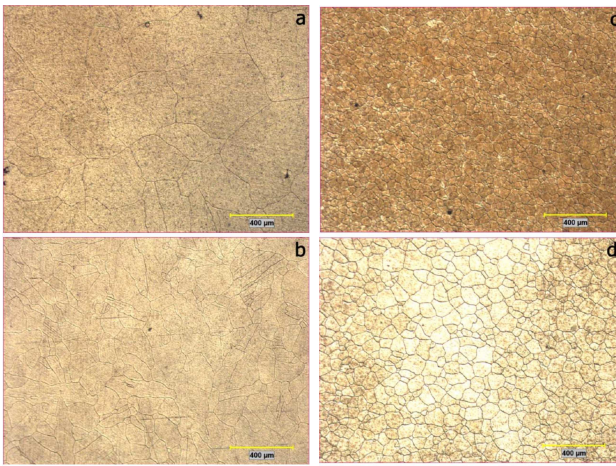
Fig. 3. Optical micrographs of heat treated Mg–Sn–Mn ternary alloys: (a) alloy 1, (b) alloy 2, (c) alloy 3, and (d) alloy 4.

Fig. 4. SEM images of as-cast Mg-Sn-Mn ternary alloys: (a) alloy 1, (b) alloy 2, (c) alloy 3, and (d) alloy 4.
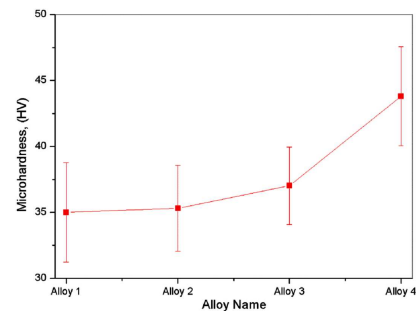
Fig. 5. The microhardness profiles of as-cast Mg-Sn-Mn ternary alloys.

ilar to that of obtained by optical microscopy (Fig. 3). There was light grey color precipitates located on the arms of the dendrites while a smaller number of those precipitates were formed between dendrites arms. It was reported in similar literature that the dendrites arms were rich in Sn [20]. Therefore, it is thought that these precipitates could be intermetallic Mg_2Sn when XRD results and SEM images are interpreted together.

The microhardness profiles of the Mg–Sn–Mn ternary alloys are shown in Fig. 5. The average microhardness values are not significantly changed but it seems that the microhardness values slightly increase with the increase of Mn content in as-cast Mg–Sn–Mn ternary alloys. The average microhardness values of the alloy 1, alloy 2, alloy 3 and alloy 4 are approximately 35, 35.5, 37, and 44 HV, respectively.

4. Conclusion

1. Mg phase is evident for the as-cast alloys while Mg_2Sn intermetallic phase is detected for alloy 2, alloy 3 and alloy 4 in addition to Mg phase after the heat treatment.

2. The dendritic microstructure changed to equiaxed grain structure after the heat treatment of Mg–Sn–Mn alloys.

3. The grain size of the ternary alloys decreased with the increasing amount of manganese content in the alloys.

4. Sn-rich precipitates were formed on dendrite arms and between dendrites while dendrites of as-cast alloys while their concentration was much higher on the dendrite arms.

5. The microhardness of the alloys increased slightly with the increase of Mn in the alloys.

References

[1] M.K. Kulekci, *Int. J. Adv. Manuf. Technol.* **39**, 851 (2008).

[2] H.M. Aichinger, *Stahl Eisen* **116**, 71 (1996).

[3] J. Liang, B.G. Guo, J. Tian, H.W. Liu, J.F. Zhou, W.M. Liu, T. Xu, *Surf. Coat. Technol.* **199**, 121 (2005).

[4] A.L. Yerokhin, A. Shatrov, V. Samsonov, P. Shashkov, A. Leyland, A. Matthews, *Surf. Coat. Technol.* **182**, 78 (2004).

[5] H.P. Duan, K.Q. Du, C.W. Yan, F.H. Wang, *Electrochim. Acta* **51**, 2898 (2006).

[6] R. Montoya, M.L. Escudero, M.C. Garcia-Alonso, *Mater. Sci. Eng. B* **176**, 1807 (2011).

[7] M. Alvarez-Lopez, M.D. Pereda, J.A. del Valle, M. Fernandez-Lorenzo, M.C. Garcia-Alonso, O.A. Ruano, M.L. Escudero, *Acta Biomater.* **6**, 1763 (2010).

[8] Z.J. Li, X.N. Gu, S.Q. Lou, Y.F. Zheng, *Biomaterials* **29**, 1329 (2008).

[9] Z.P. Yao, L.L. Li, Z.H. Jiang, *Appl. Surf. Sci.* **255**, 6724 (2009).

[10] S. Shadanbaz, G.J. Dias, *Acta Biomater.* **8**, 20 (2012).

[11] A. Seyfoori, S. Mirdamadi, A. Khavandi, Z.S. Raufi, *Appl. Surf. Sci.* **261**, 92 (2012).

[12] Y.C. Li, C. Wen, D. Mushahary, R. Sravanthi, N. Harishankar, G. Pande, P. Hodgson, *Acta Biomater.* **8**, 3177 (2012).

[13] Y.L. Zhou, J. An, D.M. Luo, W.Y. Hu, Y.C. Li, P. Hodgson, C.E. Wen, *Mater. Technol.* **27**, 52 (2012).

[14] V. Rondeau, D. Commenges, H. Jacqmin-Gadda, J.F. Dartigues, *Am. J. Epidemiol.* **152**, 59 (2000).

[15] S.S. Abd El-Rahman, *Pharmacol. Res.* **47**, 189 (2003).

[16] H.M. Liu, Y.G. Chen, Y.B. Tang, S.H. Wei, G. Niu, *J. Alloys Comp.* **440**, 122 (2007).

[17] C. Zhao, F. Pan, S. Zhao, H. Pan, K. Song, A. Tang, *Mater. Sci. Eng. C* **54**, 245 (2015).

[18] E.L. Zhang, D.S. Yin, L.P. Xu, L. Yang, K. Yang, *Mater. Sci. Eng. C* **29**, 987 (2009).

[19] L.P. Xu, G.N. Yu, E. Zhang, F. Pan, K. Yang, *J. Biomed. Mater. Res. A* **83**, 703 (2007).

[20] M.B. Yang, C.Y. Qin, F.S. Pan, *Trans. Nonferr. Met. Soc. China* **21**, 2168 (2011).